Electronic Supplementary Material (ESI) for Dalton Transactions.
This journal is © The Royal Society of Chemistry 2015

Supporting Information

Intraprotein transmethylation via a CH_3–Co(III) species in myoglobin reconstituted with a cobalt corrinoid complex

Yoshitsugu Morita,[a] Koji Oohora,[ab] Akiyoshi Sawada,[c] Kazuki Doitomi,[c] Jun Ohbayashi,[a] Takashi Kamachi,[c] Kazunari Yoshizawa,[cd] Yoshio Hisaeda[e] and Takashi Hayashi[*a]

[a]*Department of Applied Chemistry, Graduate School of Engineering, Osaka University, Suita 565-0871, Japan*

[b]*Frontier Research Base for Global Young Researchers, Graduate School of Engineering, Osaka University, Suita 565-0871, Japan*

[c]*Institute for Materials Chemistry and Engineering and International Research Centre for Molecular Systems, Kyushu University, Nishi-ku, Fukuoka 819-0395, Japan*

[d]*Elements Strategy Initiative for Catalysts and Batteries (ESICB), Kyoto University, Nishikyo-ku, Kyoto 615-8520, Japan*

[e]*Department of Chemistry and Biochemistry, Graduate School of Engineering, Kyushu University, Fukuoka 819-0395, Japan*

Contens:

Instruments 1

HPLC analysis for the kinetics of the transmethylation. 2

Reference 23

Instruments

UV-vis spectral measurements were carried out with a Shimadzu UV-3150 or UV-2550 double-beam spectrophotometer, or a Shimadzu BioSpec-nano spectrometer. ESI-TOF MS and MALDI-TOF MS analyses were performed with a Bruker Daltonics micrOTOF mass spectrometer and a Bruker autoflex III smartbeam mass spectrometer, respectively. ^{1}H and ^{13}C NMR spectra were collected on a Bruker BioSpin DPX400 (400 MHz) or a Varian Unity Inova 600 MHz NMR spectrometer. The ^{1}H and ^{13}C NMR chemical shift values are reported in ppm relative to a residual solvent peak. ICP-OES (inductively coupled plasma optical emission spectroscopy) was performed on a Shimadzu ICPS-7510 emission spectrometer. EPR spectra were measured using a Bruker EMX Plus spectrophotometer at the Instrument Center of the Institute for Molecular Science (Okazaki, Japan). CD spectra were recorded at 25 °C on a JASCO spectropolarimeter (Model J-820). The pH measurements were made with an F-52 Horiba pH meter. Air-sensitive manipulations were performed in a UNILab glove box (MBraun, Germany).

HPLC analysis for the kinetics of the transmethylation.

The transmethylations reactions of native myoglobin and rMb(Co(TDHC)) were evaluated by HPLC analysis.

Native myoglobin: The solution of native myoglobin (25 μM, 3 mL) in 0.1 M potassium phosphate buffer solution (pH 7.0) was reduced with 30 μL of 10 mg/mL sodium dithionite (54.8 mM) in the same buffer solution and then methyl iodide (3 μL) was added. At desired reaction times (0, 3, 7, 12, 24, 48 h), the protein solution (25 μM, 0.5 mL) was passed through a PD MiniTrap G-25 column (GE Healthcare) equilibrated with 50 mM Tris-HCl buffer (pH 8) containing 6 M guanidine HCl at 4 ºC. The buffer was exchanged to 50 mM Tris-HCl buffer (pH 7.6) containing 1 mM $CaCl_2$ using the same gel filtration column and the solution was concentrated to 50 μL using an Amicon Ultra-4 Centrifugal Filter (10 kDa) (GE Healthcare). To the solution, Sequencing Grade Modified Trypsin (Promega) (0.05 mg/mL, 1 μL) was added and the mixture was incubated at 37 ºC overnight.

rMb(Co^{II}(TDHC)): The protein (25 μM, 5 mL) in 0.1 M potassium phosphate buffer solution (pH 7.0) was reduced with 50 μL of 10 mg/mL sodium dithionite (54.8 mM) in the same buffer solution and then methyl iodide (5 μL) was added. At desired reaction times (0, 6, 12, 24, 48 h), each protein solution (12.5 μM, 1 mL) was dissolved in 4 mL of 17 mM Tris-HCl buffer (pH 8) containing 1 M guanidine HCl at 4 ºC. After concentration to 0.5 mL, the protein solution was passed through the same gel filtration column equilibrated with 17 mM Tris-HCl buffer (pH 7.5) containing 1 M guanidine HCl at 4 ºC. The buffer was exchanged to 50 mM Tris-HCl buffer (pH 7.6) containing 1 mM $CaCl_2$ and concentrated until 50 μL using the same centrifugal filter. To each solution, Sequencing Grade Modified Trypsin (Promega) (0.5 mg/mL, 1 μL) was added and the mixture was incubated at 37 ºC for 2 h.

The solutions containing the peptide fragments were analyzed by HPLC with a YMC-Pack Pro C18 column. The analysis was performed at a flow rate of 1 mL/min of 75% or 78% water/acetonitrile co-solvent containing 0.1% TFA for 40 or 70 min in a column oven at 60 ˚C (Fig. S10 and 5a), respectively. Each fraction was characterized by ESI-TOF-MS.

The fractions of the peaks located at about 56 and 58 min in Fig. 5a were assigned to the peptide containing non-methylated His64, HGTVVLTALGGILK, and the peptide containing methylated His64, H(CH_3)GTVVLTALGGILK, by ESI-TOF MS. Found m/z = 1378.813 (56 min) and 1392.829 (58 min), calculated m/z = 1378.841 (z = 1+) and 1392.857 (z = 1+). The concentration of the methylated peptide was determined from the ratio of peak areas of methylated and non-methylated peptides.

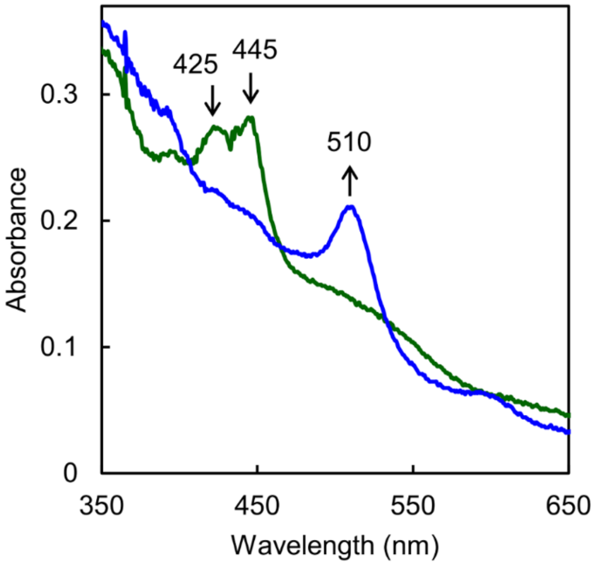

Fig. S1. The spectral changes of rMb(CH_3–Co^{III}(TDHC)) species induced by photo-irradiation over 90 sec in the aqueous solution containing 4-hydroxy-TEMPO as a radical quencher. Green and blue spectra represents the initial and final stages of the photoreaction, respectively. The aqueous solution was irradiated by a 500 W xenon arc lamp (Ushio Optical Modulex, SX-U1501XQ) filtered with cut-off filters (Asahi Spectra, Super cold filter 5C0751 and HOYA CANDEO OPTONICS, Sharp cut filter L42). The illuminance of the irradiated light from 420 nm to 800 nm monitored by a luminometer (MINOLTA, Illuminance meter T-10P) was 1.8×10^5 lux. Conditions: [protein] = 0.024 mM and [4-hydroxy-TEMPO] = 0.038 mM in 0.1 M potassium phosphate buffer (pH 7.0) at 25 °C under N_2 atmosphere.

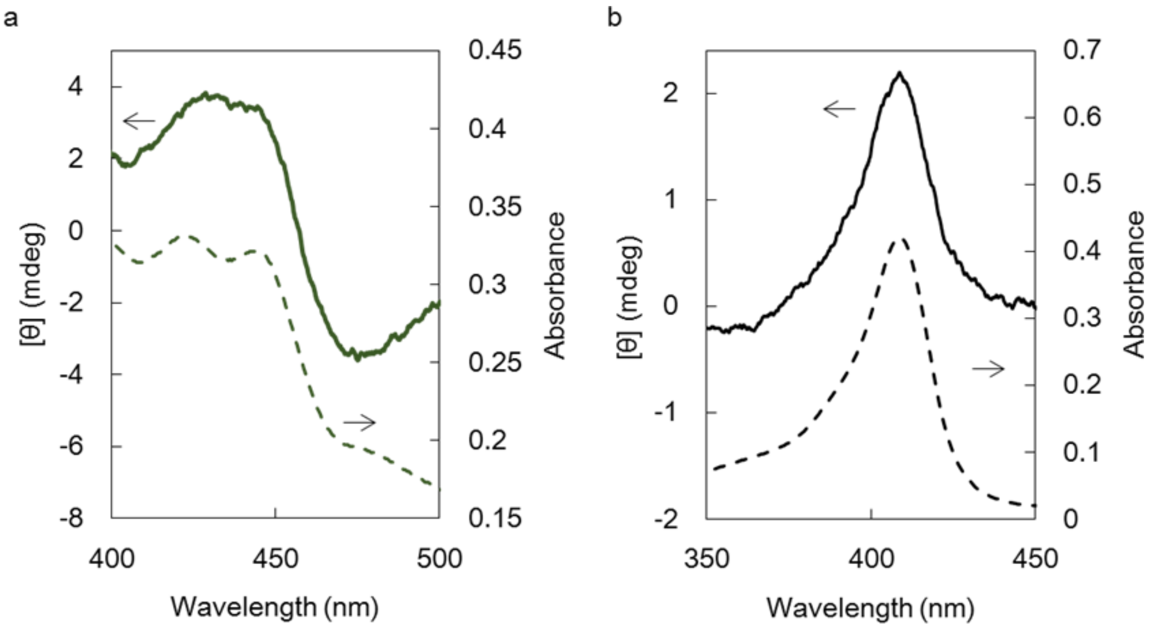

Fig. S2. The CD and UV-vis spectra of (a) rMb(CH_3−Co^{III}(TDHC)) and (b) native myoglobin in the visible region. Solid and dashed lines represent CD and UV-vis spectra, respectively. Conditions: (a) [rMb(CH_3−Co^{III}(TDHC))] = 0.023 mM in 0.1 M potassium phosphate buffer (pH 7.0) at 25 ºC under N_2 atmosphere, (b) [native myoglobin] = 0.0020 mM in the same buffer at 25 °C.

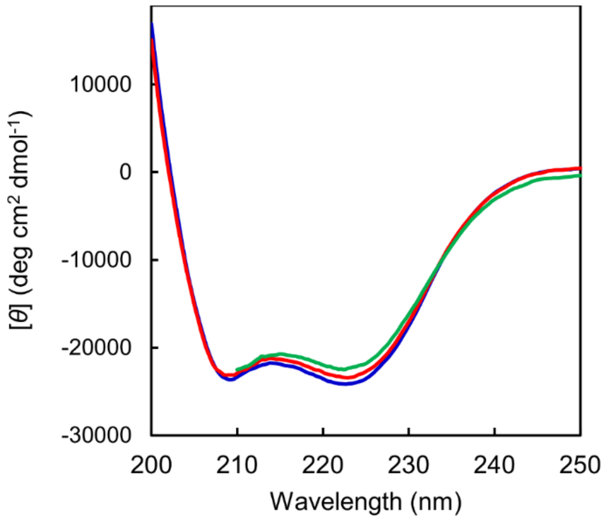

Fig. S3. Circular dichroism (CD) spectra of rMb(Co^{II}(TDHC)) (blue), rMb(Co^{I}(TDHC)) (red) and rMb(CH_3−Co^{III}(TDHC)) (green). Conditions: [protein] = 0.018 mM in 0.1 M potassium phosphate buffer (pH 7.0) at 25 °C under N_2 atmosphere. In the case of rMb(CH_3−Co^{III}(TDHC)), the region of the spectrum below 210 nm is omitted due to the strong absorption of excess methyl iodide in this region.

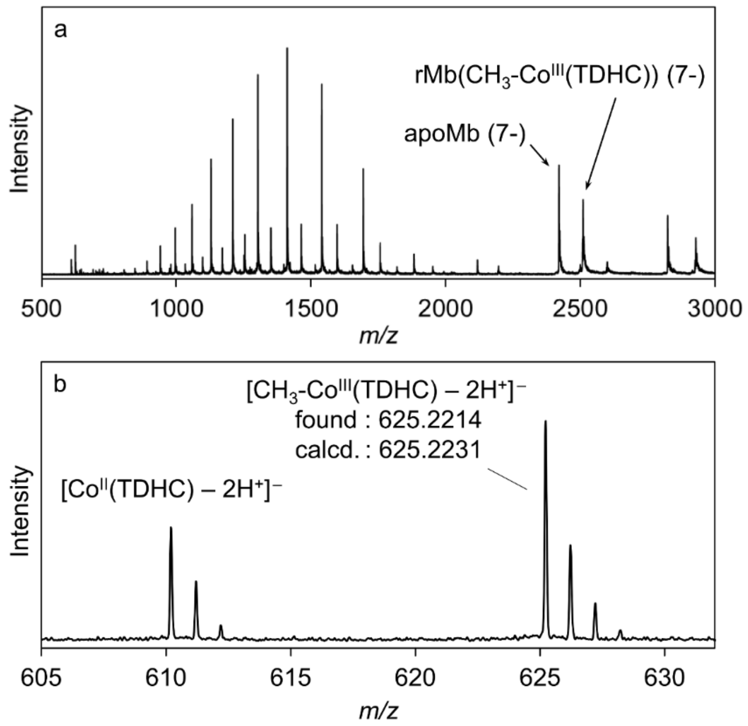

Fig. S4. ESI mass spectra (negative mode) of the reaction sample, rMb(CH$_3$−Co^{III}(TDHC)), prepared by addition of methyl iodide to rMb(Co^{I}(TDHC)) at 4 °C in 0.1 M ammonium acetate buffer solution (pH 6.7): (a) the raw spectrum, and (b) the expanded spectrum. The ESI-TOF MS conditions are described below. Depending on the voltage settings in the ion sampling interface, the cofactor–protein interaction in myoglobin can be disrupted by CID (collision-induced dissociation) in the interface region of the mass spectrometer.[S1] The voltage difference between the gas capillary exit and the 1st skimmer was 20 V. The desolvation temperature was 180 ºC.

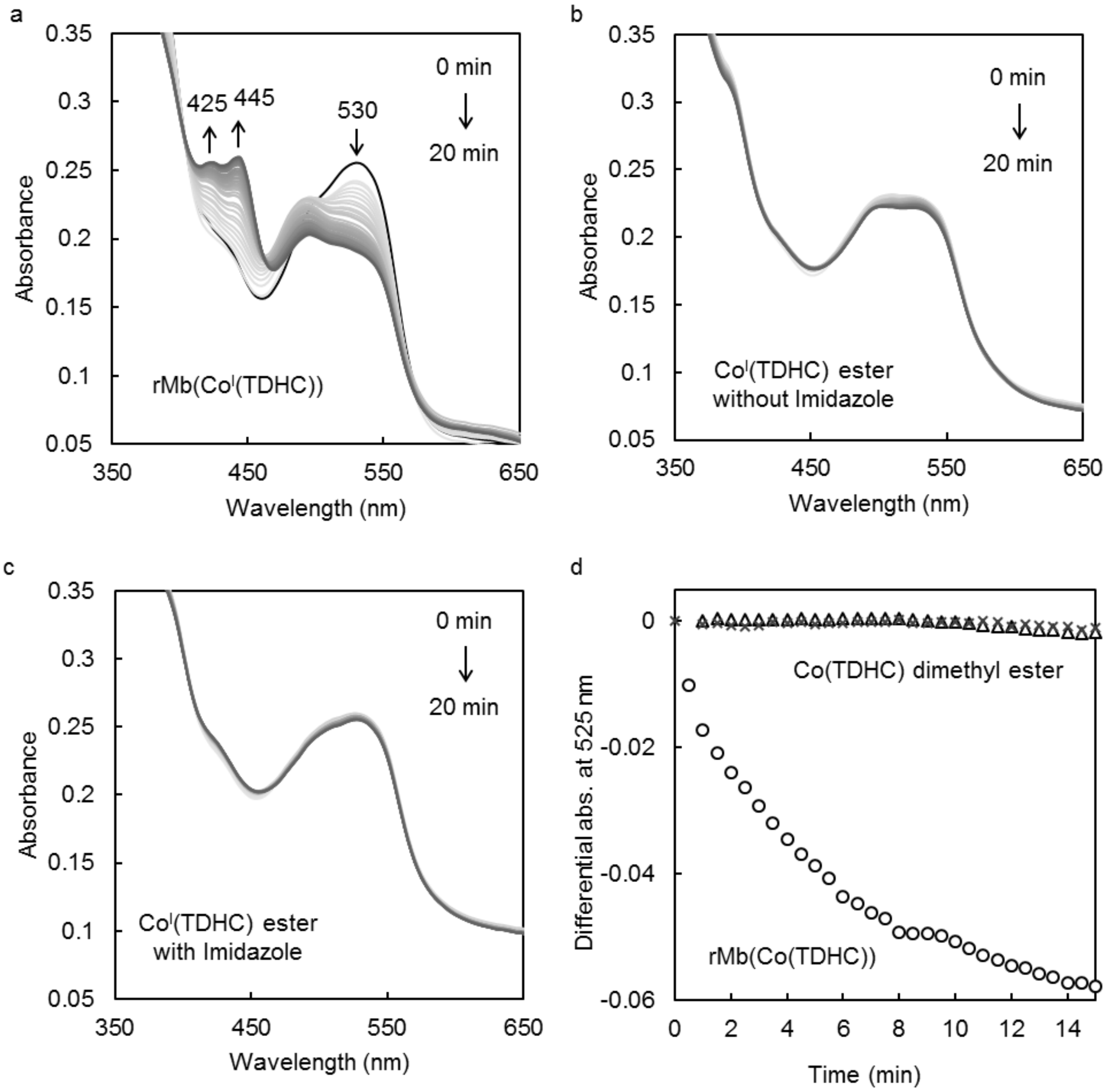

Fig. S5. UV-vis spectral changes of the Co(I) species after addition of methyl iodide until 20 min at 25 °C. (a) rMb(Co^{I}(TDHC)) in 0.1 M potassium phosphate buffer solution (pH 7); (b) Co^{I}(TDHC) dimethyl ester in CH_2Cl_2; (c) Co^{I}(TDHC) dimethyl ester in CH_2Cl_2 containing imidazole. Conditions: [Co(I) species] = 25 μM, [CH_3I] = 16 mM, [Imidazole] = 1 mM. (d) Time courses of the spectral changes of rMb(Co^{I}(TDHC)) at 525 nm (circle, ○), Co^{I}(TDHC) ester in CH_2Cl_2 (rhombus, x) and the Co(I) complex in CH_2Cl_2 containing imidazole (triangle, ▵) at 25 °C. Conditions: [Co(I) species] = 25 μM, [CH_3I] = 16 mM, [imidazole] = 1 mM.

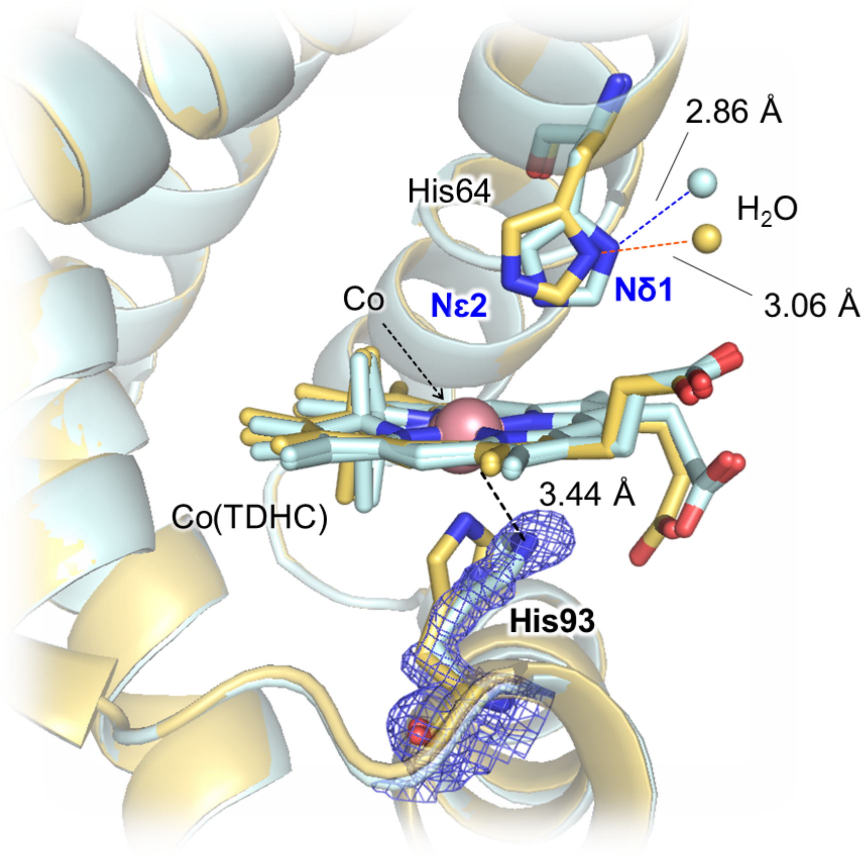

Fig. S6. Crystal structures of two oxidation states of the reconstituted protein.[S2] The cofactors and the heme pocket residues of rMb(Co^I(TDHC)) (light blue) and rMb(Co^{II}(TDHC)) (yellow) are superimposed. The $2F_o - F_c$ electron density is shown as a blue grid (contoured at 1.0 σ) around the His93 residue of rMb(Co^I(TDHC)).

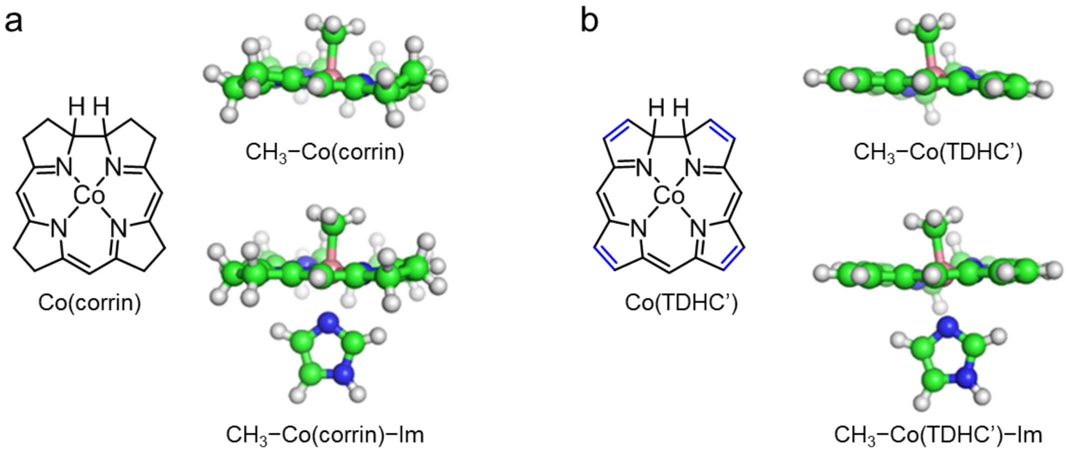

Fig. S7. Structure of (a) Co(corrin) and (b) Co(TDHC') optimized by DFT calculations.

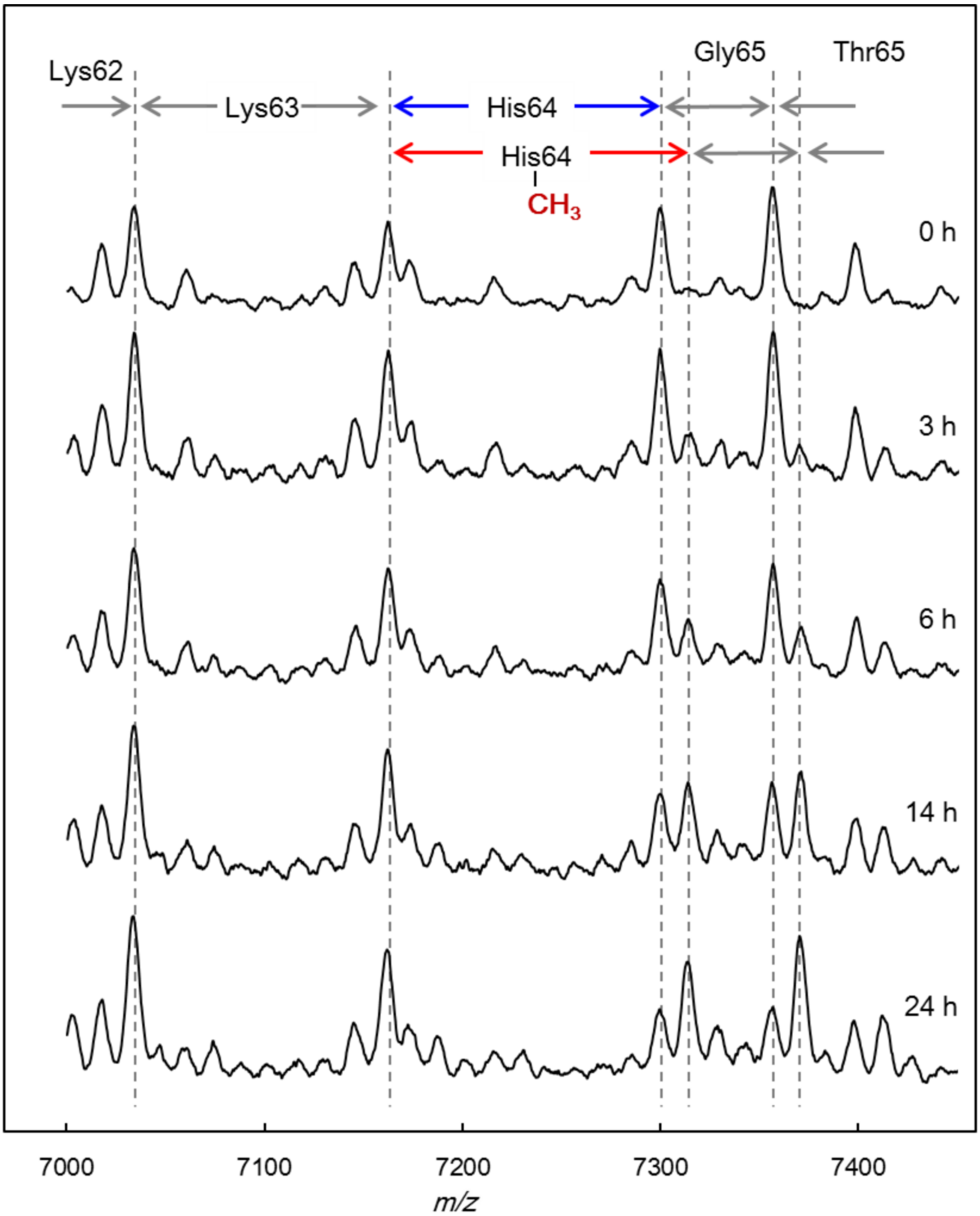

Fig. S8. MALDI-TOF MS (in-source decay mode) spectra of rMb(CH_3−Co^{III}(TDHC)) treated with methyl iodide after the reaction for 0, 3, 6, 14 and 24 h.

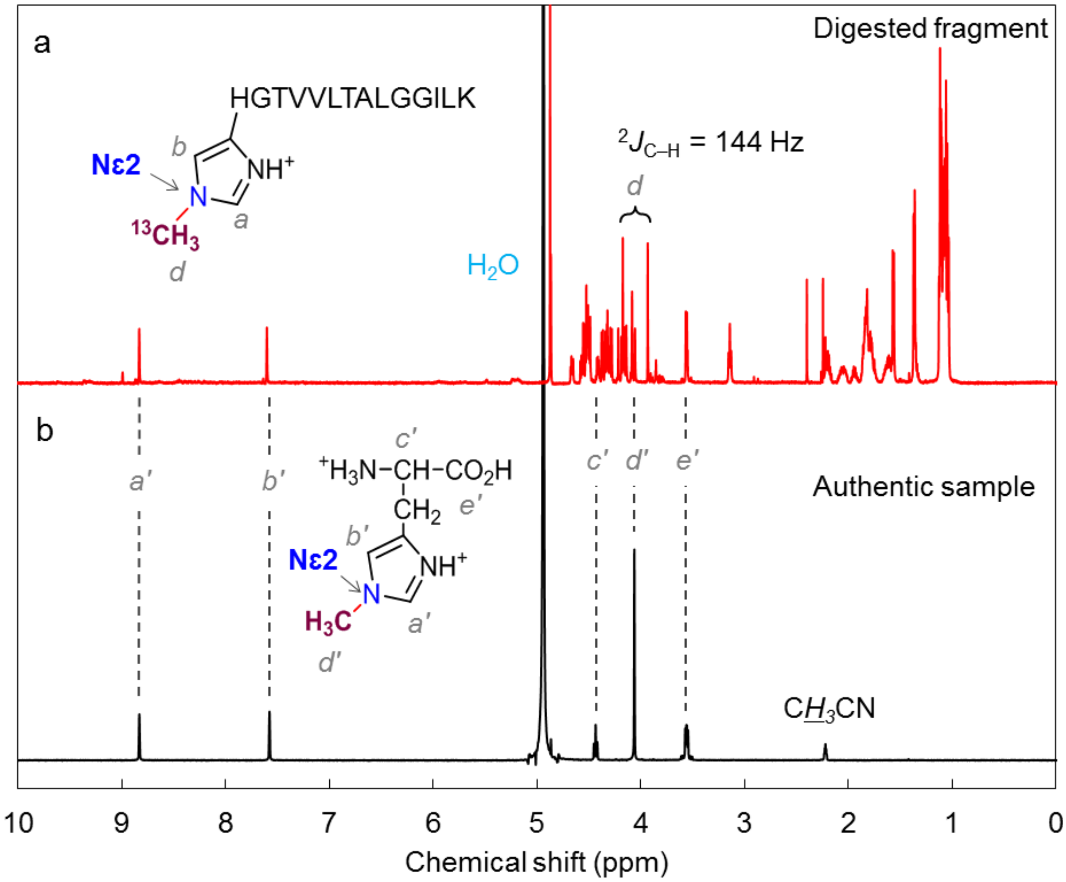

Fig. S9. (a) ^{1}H NMR (600 MHz, D_2O/CD_3CN (9:1)) spectrum of the peptide of H($^{13}CH_3$)GTVVLTALGGILK and (b) ^{1}H NMR (400 MHz, D_2O/CD_3CN (9:1) containing 1% TFA) spectrum of Nε2-methylated histidine as an authentic sample.

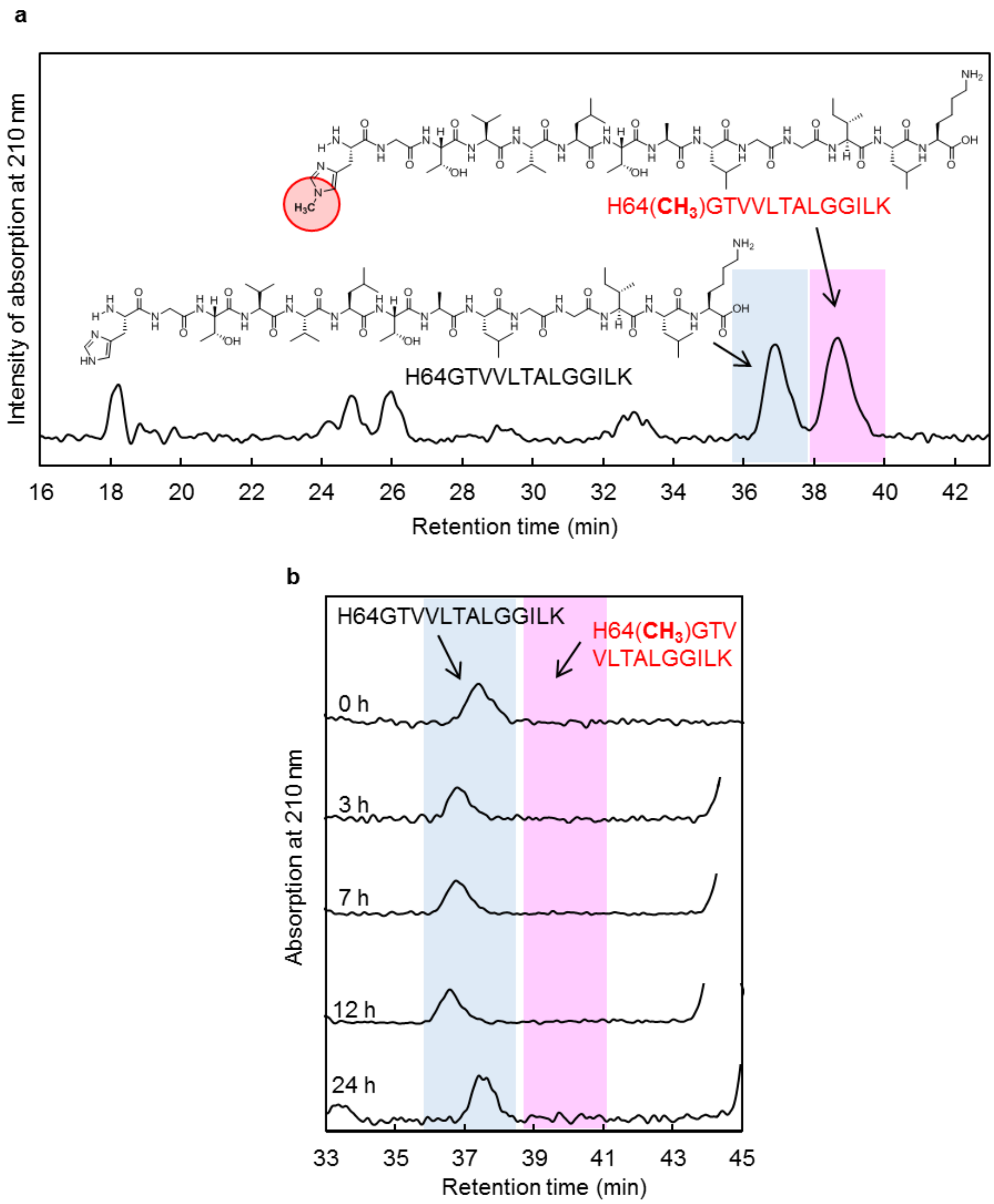

Fig. S10. (a) The HPLC trace for the mixture of the digested peptides including normal His64 and the Nε-methyl His64, which was obtained by the transmethylation. (b) The HPLC traces for the digested peptides of native myoglobin after the reaction in 0.1 M potassium phosphate buffer solution (pH 7) at 25 °C for several hours. The reaction times are indicated in each trace. The analysis was performed at a flow rate of 1 mL/min of 75% water/acetonitrile co-solvent containing 0.1% TFA for 40 min using a column oven at 60 ˚C. The fractions of the peaks around 37 and 38 min were assigned to the peptide containing methylated and non-methylated HGTVVLTALGGILK by ESI-TOF MS, respectively.

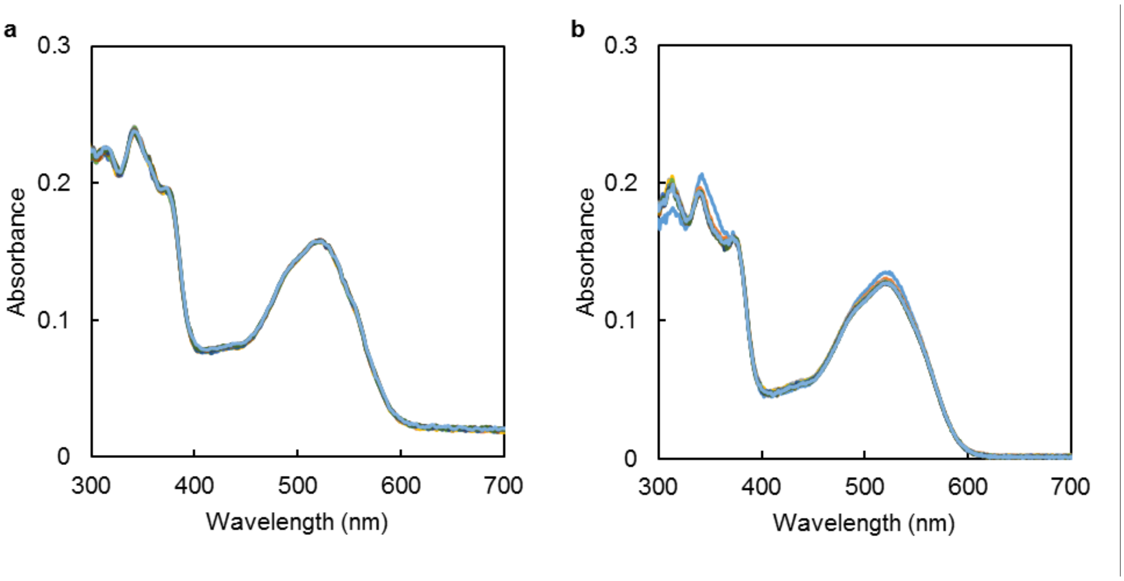

Fig. S11. UV-vis spectra of methylcobalamin in 0.1 M potassium phosphate buffer solution (pH 7.0) upon addition of each amino acid: (a) histidine or (b) cysteine until 12 h at 25 °C. Conditions: [methylcobalamin] = 16 μM, [His] = [Cys] = 25 μM.

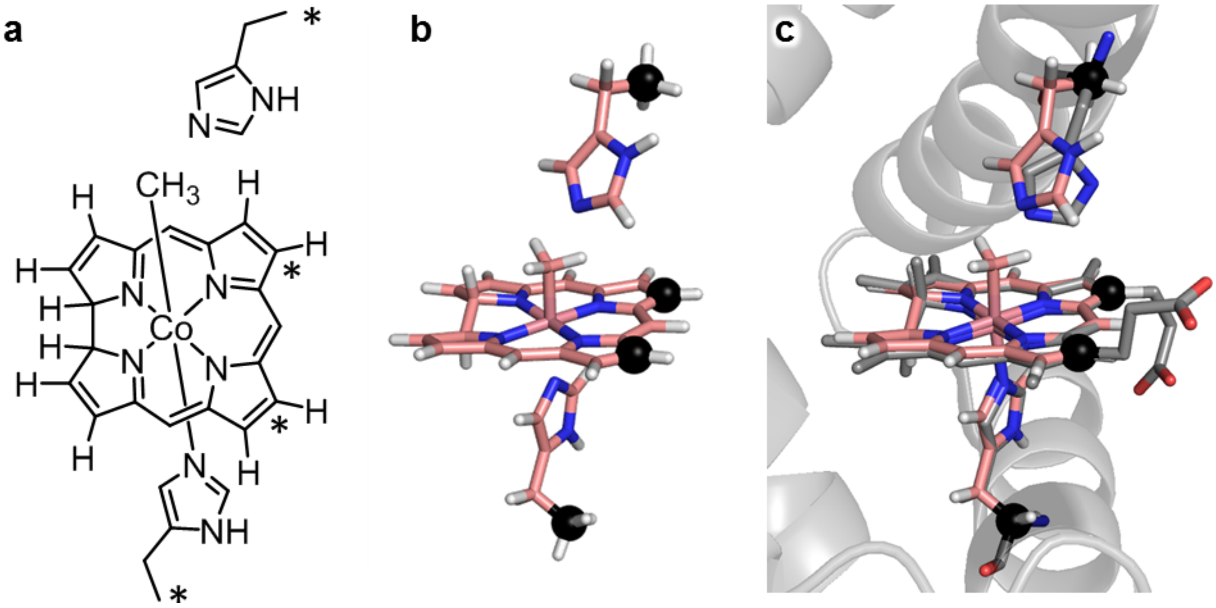

Fig. S12. (a) Schematic structure of Co(TDHC') used for DFT calculations**.** The asterisks identify the fixed carbon atoms to retain the structure of the active site. (b) Optimized structure of CH_3–Co(TDHC') (RC) and (c) a superimposition of Co(TDHC') (pink) and rMb(Co(TDHC)) (PDB ID: 3WFT) (gray) structures. The fixed atoms are shown as black spheres.

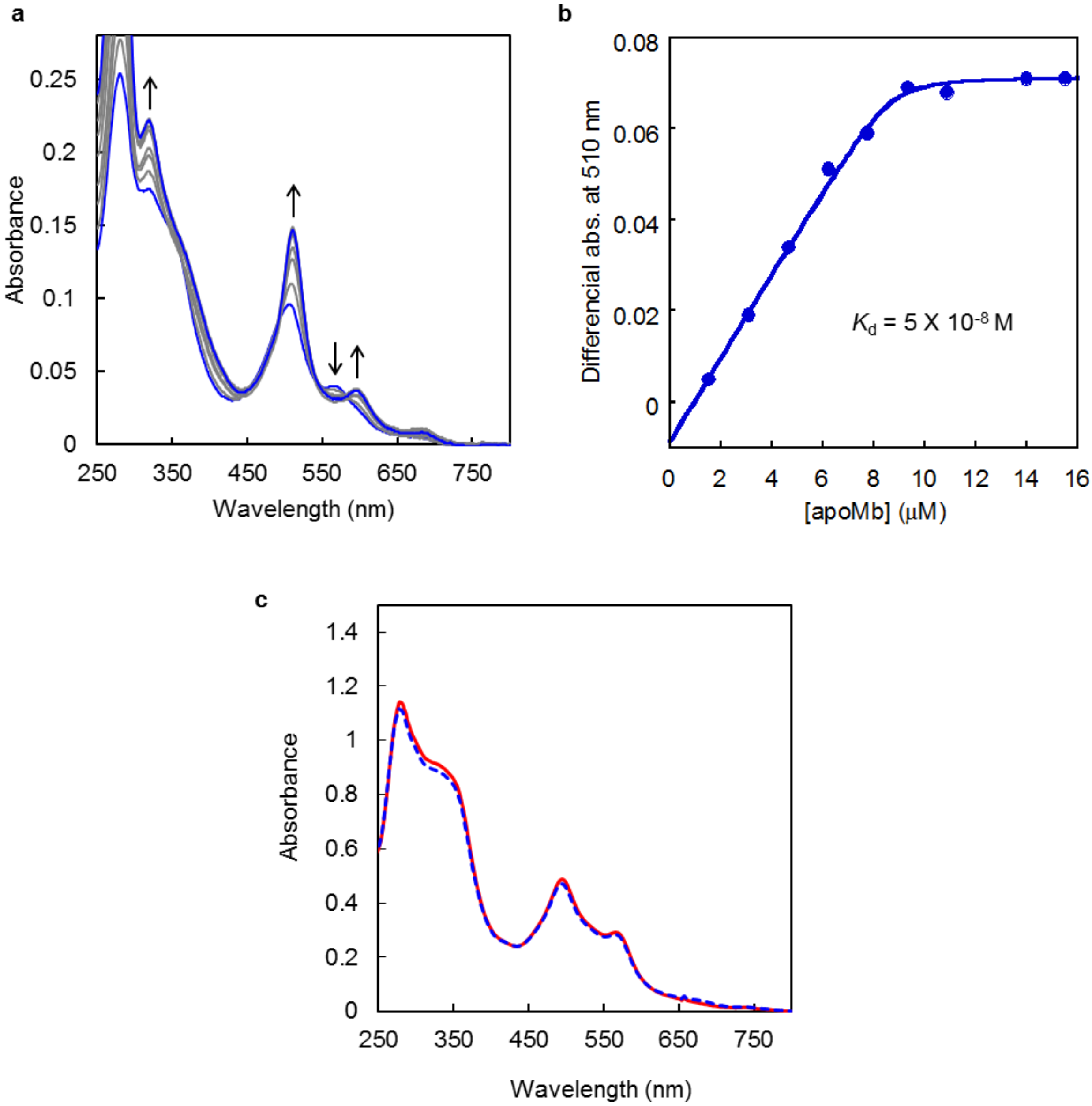

Fig. S13. (a) UV-vis spectral changes of the Co^{II}(TDHC) (8.7 μM) at various concentrations of apoMb (1.55−15.5 μM) in 0.1 M potassium phosphate buffer solution (pH 7.0) at 25 ˚C. (b) The plots of absorption at 510 nm against concentrations of apoMb with a fitting curve to determine the dissociation constant (K_d). (c) UV-vis spectra of Co^{II}(TDHC) (50 μM) under the same conditions in the absence (red solid line) and presence of imidazole (1 mM) (blue dashed line).

Table S1. DFT-computed homolytic bond-dissociation energy (BDE) and stabilization energy induced by coordination of imidazole in the gas phase.

cobalt complex	BDE (kcal/mol)			stabilization by the axial coordination (kcal/mol)[e]	
	Im-coordinated CH_3−Co(III) complex[a]		Im-free CH_3−Co(III) complex[d]	CH_3−Co(III) complex	Co(II) complex
Co(corrin)	36.4[b]	58.2[c]	42.3	15.9	21.8
Co(TDHC')	32.5[b]	56.1[c]	41.8	14.3	23.6

[a] Two cases of homolytic BDE of the imidazole-coordinated CH_3−Co(III) complex were calculated. [b] The methylated complex is split into two fragments, a methyl radical and a corresponding penta-coordinated Co(II) complex with imidazole as an axial ligand. Thus, the BDE of CH_3−Co in the methylated complex (hexa-coordination) was determined. [c] In contrast, the methylated complex is split into three fragments, a methyl radical, imidazole, and a corresponding tetra-coordinated Co(II) complex. Thus, the BDE of the methylated complex (hexa-coordination) includes dissociation of CH_3−Co and Co−Im bonds. [d] The BDE of the Co−CH_3 bond in the methylated complex (penta-coordination) was determined. [e] The stabilization energy was evaluated by the BDE value of the Co−N(Im) bond in the each imidazole-coordinated complex. The energy diagram for the homolytic dissociation is illustrated below.

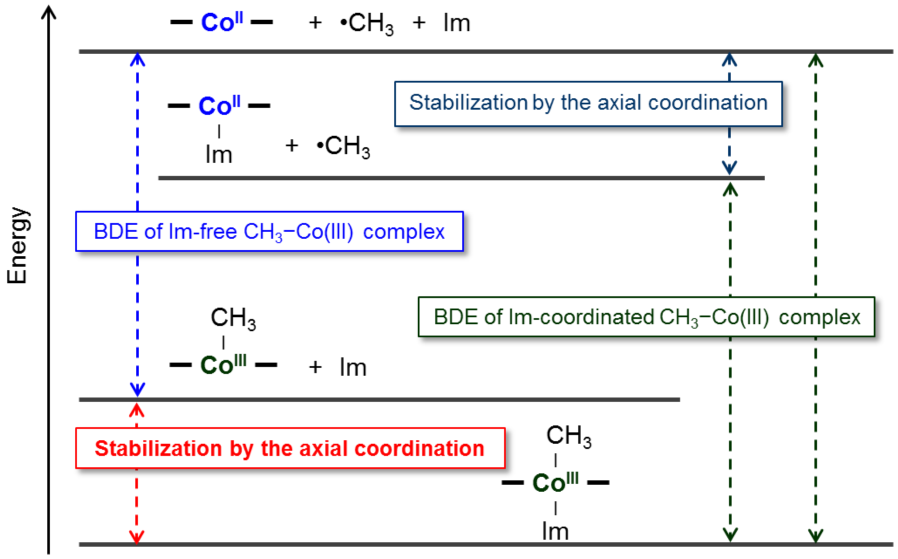

Table S2. Cartesian coordinates for the optimized structure of the reaction complex (RC).

C	0.381373	4.162653	1.141637
C	0.800385	3.612177	2.323176
C	0.836120	2.169769	2.134539
N	0.441244	1.869682	0.822200
C	0.138614	3.073448	0.221790
C	1.206839	1.217986	3.080111
C	1.308836	-0.161496	2.760864
N	1.007634	-0.598509	1.523920
C	1.374271	-2.017331	1.409294
C	1.742398	-2.412812	2.805642
C	1.761635	-1.290471	3.578274
C	0.199256	-2.622393	0.587086
N	-0.081933	-1.571960	-0.408394
C	-0.266924	-2.141900	-1.609844
C	-0.027213	-3.587194	-1.511517
C	0.307143	-3.880766	-0.227599
C	-0.619557	-1.361094	-2.740809
C	-0.714127	0.024326	-2.683702
C	-1.077280	0.911297	-3.779145
C	-1.008634	2.192165	-3.301929
C	-0.594960	2.112523	-1.917617
N	-0.422451	0.793783	-1.546303
C	-0.353631	3.198471	-1.077400
Co	0.102193	0.159062	0.135873
C	-1.659009	0.236893	1.001272
C	4.680698	-0.416105	0.318245
C	5.846548	-0.151022	-0.381938
N	5.828955	-1.073078	-1.425131
C	4.693893	-1.833150	-1.311819
C	6.935262	0.865457	-0.188559
C	6.887538	2.045062	-1.186400
N	-4.418454	-1.476089	0.129344
C	-5.072788	-0.481557	-0.583161
C	-6.378714	-0.315194	-0.148554
N	-6.513119	-1.252119	0.872680
C	-5.319546	-1.919342	0.999520
C	-7.472898	0.631718	-0.550304
C	-7.738884	1.756557	0.476523
H	-8.539360	2.427862	0.119967
H	-8.054139	1.348752	1.453670
H	-6.829592	2.359231	0.643166
H	-8.411499	0.072830	-0.737122
H	-7.190754	1.078938	-1.520371
H	-7.359646	-1.424383	1.413890
H	-4.569041	0.065200	-1.381560
H	-5.169780	-2.714348	1.730686
H	7.701460	2.760326	-0.977303
H	7.002668	1.701246	-2.229897
H	5.926597	2.582603	-1.114015
H	7.925769	0.372310	-0.244741
H	6.850718	1.253536	0.842256

H	6.549304	-1.175028	-2.139426
H	4.317345	0.087434	1.214293
H	4.450079	-2.637409	-2.005527
H	-0.544747	4.204177	-1.463077
H	-0.822318	-1.862393	-3.691277
H	-0.112115	-4.282534	-2.349518
H	0.519691	-4.867499	0.188414
H	-0.679535	-2.697294	1.262484
H	2.299002	-2.057406	0.759640
H	2.075709	-3.411006	3.096971
H	2.076141	-1.210588	4.621196
H	1.469029	1.554315	4.087310
H	-1.498027	0.219357	2.091127
H	-2.123051	1.186262	0.693704
H	-2.266447	-0.615817	0.658712
H	-1.337814	0.577009	-4.784375
H	-1.205036	3.121641	-3.838757
H	0.243295	5.218623	0.903837
H	1.078274	4.123104	3.246127
N	3.970806	-1.458246	-0.260474

Table S3. Cartesian coordinates for the optimized structure of the transition state (TS1) of deligation of imidazole in the stepwise pathway.

C	0.897200	3.771321	1.830367
C	1.161760	2.983442	2.918539
C	1.026919	1.599517	2.487533
N	0.691825	1.575910	1.126250
C	0.585986	2.890493	0.726620
C	1.196925	0.463245	3.276049
C	1.128101	-0.846097	2.731694
N	0.845964	-1.026359	1.431089
C	1.017769	-2.444592	1.084373
C	1.257053	-3.115611	2.406762
C	1.373613	-2.151111	3.359769
C	-0.195605	-2.729300	0.146208
N	-0.255005	-1.507991	-0.676036
C	-0.439411	-1.847296	-1.959644
C	-0.425003	-3.310511	-2.088776
C	-0.224323	-3.848238	-0.857123
C	-0.596231	-0.853158	-2.961681
C	-0.493485	0.504137	-2.680931
C	-0.663960	1.599356	-3.625247
C	-0.449263	2.762714	-2.937194
C	-0.133260	2.401547	-1.571850
N	-0.168198	1.031325	-1.421719
C	0.200021	3.292489	-0.551734
Co	0.168774	0.065441	0.145155
C	-1.608798	0.278420	0.953070

C	4.174977	-0.208086	0.138224
C	5.463876	-0.149702	-0.368177
N	5.373180	-0.809021	-1.591433
C	4.077568	-1.223582	-1.762422
C	6.740001	0.435773	0.166989
C	7.319567	1.597121	-0.671668
N	-4.404947	-1.375244	0.021931
C	-4.969193	-0.305604	-0.658818
C	-6.237377	-0.008093	-0.184601
N	-6.443355	-0.941884	0.827492
C	-5.324933	-1.734250	0.911370
C	-7.231890	1.059809	-0.539767
C	-7.344470	2.188590	0.511004
H	-8.074780	2.949917	0.186339
H	-7.677498	1.801030	1.490517
H	-6.369953	2.684345	0.660819
H	-8.231002	0.610607	-0.707699
H	-6.928870	1.491068	-1.510742
H	-7.289108	-1.033093	1.389287
H	-4.431660	0.197756	-1.463679
H	-5.241674	-2.552565	1.627268
H	8.240450	1.986697	-0.205089
H	7.578691	1.274013	-1.696119
H	6.595744	2.425881	-0.754060
H	7.505210	-0.359971	0.268932
H	6.535997	0.789434	1.193459
H	6.141719	-0.959961	-2.244060
H	3.816361	0.198516	1.084203
H	3.747125	-1.768412	-2.646647
H	0.167456	4.364096	-0.769100
H	-0.808568	-1.162149	-3.989000
H	-0.558262	-3.846462	-3.031142
H	-0.194093	-4.908646	-0.599150
H	-1.110472	-2.770251	0.773988
H	1.931675	-2.500501	0.449433
H	1.429632	-4.186106	2.535184
H	1.625254	-2.290632	4.413468
H	1.432667	0.591006	4.336355
H	-1.492768	0.203908	2.046155
H	-1.970843	1.278151	0.668309
H	-2.278755	-0.503893	0.563365
H	-0.908641	1.473086	-4.680871
H	-0.484428	3.785101	-3.316926
H	0.908072	4.860857	1.771427
H	1.434767	3.293977	3.928065
N	3.317516	-0.875331	-0.726873

Table S4. Cartesian coordinates for the optimized structure of the intermediate (Int) in the stepwise pathway.

C	0.381373	4.162653	1.141637
C	0.800385	3.612177	2.323176
C	0.836120	2.169769	2.134539
N	0.441244	1.869682	0.822200
C	0.138614	3.073448	0.221790
C	1.206839	1.217986	3.080111
C	1.308836	-0.161496	2.760864
N	1.007634	-0.598509	1.523920
C	1.374271	-2.017331	1.409294
C	1.742398	-2.412812	2.805642
C	1.761635	-1.290471	3.578274
C	0.199256	-2.622393	0.587086
N	-0.081933	-1.571960	-0.408394
C	-0.266924	-2.141900	-1.609844
C	-0.027213	-3.587194	-1.511517
C	0.307143	-3.880766	-0.227599
C	-0.619557	-1.361094	-2.740809
C	-0.714127	0.024326	-2.683702
C	-1.077280	0.911297	-3.779145
C	-1.008634	2.192165	-3.301929
C	-0.594960	2.112523	-1.917617
N	-0.422451	0.793783	-1.546303
C	-0.353631	3.198471	-1.077400
Co	0.102193	0.159062	0.135873
C	-1.659009	0.236893	1.001272
C	4.680698	-0.416105	0.318245
C	5.846548	-0.151022	-0.381938
N	5.828955	-1.073078	-1.425131
C	4.693893	-1.833150	-1.311819
C	6.935262	0.865457	-0.188559
C	6.887538	2.045062	-1.186400
N	-4.418454	-1.476089	0.129344
C	-5.072788	-0.481557	-0.583161
C	-6.378714	-0.315194	-0.148554
N	-6.513119	-1.252119	0.872680
C	-5.319546	-1.919342	0.999520
C	-7.472898	0.631718	-0.550304
C	-7.738884	1.756557	0.476523
H	-8.539360	2.427862	0.119967
H	-8.054139	1.348752	1.453670
H	-6.829592	2.359231	0.643166
H	-8.411499	0.072830	-0.737122
H	-7.190754	1.078938	-1.520371
H	-7.359646	-1.424383	1.413890
H	-4.569041	0.065200	-1.381560
H	-5.169780	-2.714348	1.730686
H	7.701460	2.760326	-0.977303
H	7.002668	1.701246	-2.229897
H	5.926597	2.582603	-1.114015
H	7.925769	0.372310	-0.244741
H	6.850718	1.253536	0.842256

H	6.549304	-1.175028	-2.139426
H	4.317345	0.087434	1.214293
H	4.450079	-2.637409	-2.005527
H	-0.544747	4.204177	-1.463077
H	-0.822318	-1.862393	-3.691277
H	-0.112115	-4.282534	-2.349518
H	0.519691	-4.867499	0.188414
H	-0.679535	-2.697294	1.262484
H	2.299002	-2.057406	0.759640
H	2.075709	-3.411006	3.096971
H	2.076141	-1.210588	4.621196
H	1.469029	1.554315	4.087310
H	-1.498027	0.219357	2.091127
H	-2.123051	1.186262	0.693704
H	-2.266447	-0.615817	0.658712
H	-1.337814	0.577009	-4.784375
H	-1.205036	3.121641	-3.838757
H	0.243295	5.218623	0.903837
H	1.078274	4.123104	3.246127
N	3.970806	-1.458246	-0.260474

Table S5. Cartesian coordinates for the optimized structure of the transition state (TS2) of the transmethylation in the stepwise pathway.

C	8.060826	-0.071712	1.113579
C	7.639743	-0.726638	-0.221735
C	6.292071	-0.263375	-0.691438
N	6.091269	0.916276	-1.404490
C	5.017939	-0.758703	-0.476424
C	4.753989	1.100097	-1.599568
N	4.087226	0.088957	-1.045779
H	9.049854	-0.445444	1.428641
H	8.127080	1.026728	1.023462
H	7.334759	-0.302979	1.911101
H	8.399991	-0.526772	-1.000652
H	7.605348	-1.823971	-0.103618
H	6.829461	1.534340	-1.743410
H	4.717602	-1.662340	0.052348
H	4.319919	1.945378	-2.130399
C	-6.464505	2.293847	1.569791
C	-6.883791	1.461467	0.337171
C	-5.960490	0.314087	0.047696
N	-5.956033	-0.871378	0.777933
C	-4.929875	0.151005	-0.863483
C	-4.957162	-1.674147	0.289778
N	-4.313396	-1.081054	-0.710451
H	-7.163196	3.133848	1.727199
H	-6.460046	1.682627	2.489926
H	-5.449896	2.706581	1.436700

H	-7.920262	1.093481	0.469926
H	-6.906089	2.111725	-0.555566
H	-6.599142	-1.105712	1.533402
H	-4.601209	0.856246	-1.627295
H	-4.751315	-2.668216	0.685962
C	0.933053	-0.095736	4.103339
C	0.682923	-1.433200	3.931419
C	0.302430	-1.623921	2.542887
N	0.323732	-0.384394	1.882045
C	0.695081	0.550924	2.833920
C	0.785790	1.920176	2.585763
C	-0.054098	-2.829088	1.937745
C	-0.364062	-2.917686	0.561521
N	-0.264377	-1.835833	-0.242275
C	-0.839132	-4.066840	-0.217733
C	-1.030131	-3.672671	-1.504054
C	-0.583983	-2.241515	-1.629917
C	-1.504164	-1.091454	-2.125276
N	-0.886827	0.108852	-1.532734
C	-1.714574	-0.725514	-3.563747
C	-1.436980	0.599804	-3.711383
C	-0.933918	1.115037	-2.434656
C	-0.544740	2.425379	-2.069215
C	-0.127550	2.741419	-0.775327
C	0.202026	4.062139	-0.269437
N	0.039503	1.798103	0.251896
C	0.467417	2.507397	1.360403
C	0.559850	3.913922	1.046778
H	1.104167	2.573387	3.404051
H	-0.096537	-3.731992	2.553828
H	-0.613060	3.229462	-2.808072
H	0.347739	-2.201062	-2.235115
H	-2.511427	-1.239543	-1.638370
H	0.741087	-2.231807	4.672727
H	-1.010346	-5.062150	0.199590
H	-1.355137	-4.292523	-2.342020
H	-2.157237	-1.387687	-4.310807
H	-1.571893	1.206786	-4.609959
H	0.142691	4.981956	-0.853627
Co	-0.120223	-0.060404	0.095094
C	2.167551	0.018710	-0.609160
H	1.864515	0.585893	-1.487768
H	2.338634	0.526981	0.335782
H	2.160329	-1.068139	-0.644576
H	1.236823	0.419421	5.016321
H	0.855927	4.690453	1.754330

Table S6. Cartesian coordinates for the optimized structure of the transition state ($TS_{concerted}$) of the concerted pathway.

C	7.697488	0.787248	-1.445764
C	7.467503	0.497745	0.055071
C	6.145668	-0.163377	0.312457
N	5.936503	-1.535514	0.194932
C	4.892068	0.356730	0.580788
C	4.614234	-1.805969	0.388601
N	3.965920	-0.667380	0.629201
H	8.671779	1.282602	-1.595890
H	7.694436	-0.141506	-2.042754
H	6.909495	1.448454	-1.843878
H	8.288479	-0.127932	0.453791
H	7.498363	1.442364	0.625952
H	6.661782	-2.229363	0.009235
H	4.601746	1.395149	0.734873
H	4.175588	-2.801354	0.350758
C	-6.861699	-1.387039	-1.740589
C	-6.537997	-0.696063	-0.397984
C	-5.208197	-0.001586	-0.394575
N	-4.971255	1.204461	-1.048166
C	-3.972282	-0.350062	0.124857
C	-3.645888	1.523238	-0.894922
N	-3.008755	0.597049	-0.185609
H	-7.838426	-1.898999	-1.690444
H	-6.906069	-0.659749	-2.570883
H	-6.090664	-2.135166	-1.991758
H	-7.344553	0.018958	-0.141314
H	-6.530448	-1.447817	0.411448
H	-5.667528	1.754924	-1.549945
H	-3.720752	-1.242669	0.698924
H	-3.201080	2.425973	-1.312439
C	0.337339	2.115622	-3.398806
C	0.191155	3.188916	-2.555750
C	-0.012295	2.658756	-1.217736
N	0.012752	1.257244	-1.270977
C	0.214267	0.921394	-2.596578
C	0.260346	-0.389691	-3.072619
C	-0.222375	3.396411	-0.050017
C	-0.365940	2.782997	1.217181
N	-0.259749	1.444900	1.354979
C	-0.671384	3.386049	2.520637
C	-0.754669	2.398494	3.450836
C	-0.404768	1.094747	2.784428
C	-1.364055	-0.134285	2.738728
N	-0.885873	-0.884283	1.562464
C	-1.452954	-1.173243	3.825245
C	-1.210862	-2.390679	3.268753
C	-0.871599	-2.203025	1.851328
C	-0.573605	-3.154568	0.847460
C	-0.313415	-2.781948	-0.475540

C	-0.077507	-3.674596	-1.598060
N	-0.231165	-1.454526	-0.919314
C	0.055026	-1.512397	-2.269834
C	0.142590	-2.887785	-2.701056
H	0.456295	-0.545444	-4.138027
H	-0.272374	4.486940	-0.122356
H	-0.586069	-4.219326	1.098588
H	0.569262	0.727813	3.173966
H	-2.374327	0.262368	2.504109
H	0.217508	4.251183	-2.804598
H	-0.814096	4.457148	2.683861
H	-0.937168	2.515647	4.520985
H	-1.774515	-0.972444	4.849287
H	-1.263055	-3.362822	3.765272
H	-0.098049	-4.764168	-1.539265
Co	-0.311236	0.085689	0.150885
C	2.062289	-0.371273	0.493650
H	1.779563	-1.334245	0.915506
H	2.106888	-0.243020	-0.584379
H	2.086162	0.505442	1.136784
H	0.505548	2.126859	-4.477215
H	0.340109	-3.207622	-3.725789

Table S7. Cartesian coordinates for the optimized structure of the product (PRO).

C	8.023808	0.375410	0.610954
C	6.578220	0.765741	0.996797
C	5.526926	0.164458	0.110253
N	5.348384	-1.210492	-0.036210
C	4.578836	0.735590	-0.714266
C	4.342757	-1.465104	-0.903930
N	3.867269	-0.284717	-1.336976
H	8.736058	0.867786	1.292776
H	8.195139	-0.713288	0.688093
H	8.261369	0.687631	-0.419623
H	6.375919	0.476021	2.046208
H	6.459427	1.861958	0.954982
H	5.897031	-1.929822	0.436148
H	4.345199	1.780842	-0.901796
H	3.984291	-2.446523	-1.202915
C	-6.503376	2.737794	0.204265
C	-6.870911	1.272344	0.529412
C	-5.685524	0.356033	0.622119
N	-4.731875	0.440155	1.633450
C	-5.229423	-0.674633	-0.184519
C	-3.772587	-0.511950	1.399621
N	-4.047612	-1.210398	0.302485
H	-7.412708	3.358928	0.128032
H	-5.861046	3.180665	0.986857
H	-5.957665	2.802802	-0.752596

H	-7.455734	1.238004	1.470509
H	-7.539464	0.876961	-0.255974
H	-4.747714	1.096966	2.412449
H	-5.695840	-1.062024	-1.091084
H	-2.911457	-0.655820	2.052158
C	0.980788	1.923905	3.394002
C	0.791555	0.670280	3.922090
C	0.431173	-0.206533	2.825186
N	0.405553	0.531094	1.628697
C	0.734827	1.833913	1.975421
C	0.785666	2.890943	1.067613
C	0.123478	-1.566855	2.915645
C	-0.192300	-2.342085	1.780582
N	-0.164808	-1.797718	0.538571
C	-0.637285	-3.737089	1.696803
C	-0.890093	-4.040629	0.396832
C	-0.519064	-2.850409	-0.445764
C	-1.515814	-2.115336	-1.383862
N	-0.912674	-0.774057	-1.510869
C	-1.805285	-2.526253	-2.797390
C	-1.575454	-1.455806	-3.606913
C	-1.034674	-0.361350	-2.795361
C	-0.665485	0.951491	-3.161243
C	-0.199975	1.877510	-2.223306
C	0.095592	3.275725	-2.464968
N	0.042247	1.578607	-0.869037
C	0.459846	2.765424	-0.283350
C	0.489591	3.820489	-1.266626
H	1.069931	3.880156	1.440834
H	0.117759	-2.037409	3.903517
H	-0.800057	1.278619	-4.196823
H	0.379614	-3.093754	-1.052708
H	-2.479790	-1.996359	-0.815145
H	0.876857	0.356688	4.964086
H	-0.759474	-4.393952	2.561763
H	-1.220273	-5.001185	-0.003790
H	-2.256604	-3.478379	-3.084739
H	-1.769065	-1.386876	-4.680416
H	-0.019613	3.776217	-3.428075
Co	-0.114275	-0.092178	-0.050954
C	2.709659	-0.106803	-2.226431
H	2.678247	-0.936823	-2.946826
H	2.820901	0.845087	-2.763280
H	1.777579	-0.085803	-1.617417
H	1.254509	2.840236	3.920677
H	0.763860	4.856693	-1.058887

Reference

S1 O. O. Sogbein, D. A. Simmons, L. Konermann, *J. Am. Soc. Mass Spectrom.* 2000, **11**, 312−319.

S2 T. Hayashi, Y. Morita, E. Mizohata, K. Oohora, J. Ohbayashi, T. Inoue and Y. Hisaeda, *Chem. Commun.*, 2014, **50**, 12560−12563.